Observations of dust acoustic waves driven at high frequencies: Finite dust temperature effects and wave interference

Edward Thomas, Jr.[a)]
Physics Department, Auburn University, Auburn, Alabama 36849, USA

Ross Fisher and Robert L. Merlino
Department of Physics and Astronomy, The University of Iowa, Iowa City, Iowa 52245, USA

(Received 14 June 2007; accepted 30 October 2007; published online 6 December 2007)

An experiment has been performed to study the behavior of dust acoustic waves driven at high frequencies ($f > 100$ Hz), extending the range of previous work. In this study, two previously unreported phenomena are observed—interference effects between naturally excited dust acoustic waves and driven dust acoustic waves, and the observation of finite dust temperature effects on the dispersion relation. © *2007 American Institute of Physics*. [DOI: 10.1063/1.2815795]

I. INTRODUCTION

Dust acoustic (DA) waves are longitudinal low-frequency dust density disturbances that propagate in dusty plasmas.[1,2] DA waves have attracted much attention in the dusty plasma community since they are the simplest example of a dusty plasma wave in which the massive negatively charged dust particles actually participate in the wave motion. An intriguing aspect of DAWs is the fact that the propagating dust density waves can be seen and analyzed by laser light scattering from the dust particles, and the dynamics of individual particles *within the wave* can be recorded in space and time.[2,3]

The considerable ongoing experimental[3–13] and theoretical[14–18] work on DAWs indicates that this remains a vibrant area of investigation. Recently, for example, Fortov, *et al.*[8] studied DAWs that appear spontaneously in an rf inductive discharge plasma. They showed experimentally and theoretically that a necessary condition for the excitation of the DAW was the presence of a minimum dc electric field within the dust cloud. Trottenberg *et al.*[11] investigated the behavior of DAWs in a weakly ionized magnetized anodic plasma. The growth rates of the self-excited waves were measured and compared with results from kinetic theory. Piel *et al.*[10] studied obliquely propagating dust-density waves in the presence of an ion beam in a dusty plasma formed under microgravity conditions. Bandyopadhyay *et al.*[13] conducted an experimental investigation aimed at uncovering evidence of strong-coupling effects on dust acoustic waves in a dc glow discharge plasma. Schwabe *et al.*[12] investigated nonlinear highly resolved dust wave structures that were self-excited in a dusty plasma under the action of thermophoresis. The critical pressure for the onset of self-excited oscillations was determined experimentally and explained theoretically. A theoretical study of DAWs relevant to collisional dusty plasmas in planetary ring systems was recently reported by Yaroshenko *et al.*[18] With specific reference to Saturn's rings, they found that the ion drag force plays a crucial role in the stability of DAWs, and that within the corotation distance the ion drag force can be responsible for the excitation of the DAW.

In typical dusty plasmas formed in glow discharge plasmas, DAWs with frequencies ranging from a few Hz to tens of Hz can appear spontaneously, most likely due to an ion streaming instability.[14] Additionally, a dust acoustic wave can also be driven at a specified frequency in a dusty plasma due to an applied sinusoidal current on an electrode.[4,11] By synchronizing the DAW frequency and measuring the wavelength for a given frequency, the dispersion relation of the DAW can be determined experimentally.[4,11] Previous dispersion relation measurements have been limited to applied frequencies below 60 Hz. One goal of the present experiment was to extend the DAW frequency range to ~200 Hz, in order to explore the dispersion relation up to and exceeding the dust plasma frequency, ω_{pd}. As will become evident shortly, however, it was not possible to observe the predicted turnover of the dispersion curve $\omega(k)$ near ω_{pd} due to the presence of the effect of finite dust temperature T_d.

In Sec. II, we review the fluid theory of the DAW including the effects of finite T_d. The experimental setup and measurement methods are discussed in Sec. III. The measurements of the DAW dispersion relation are given in Sec. IV. A discussion of the finite T_d effects on the dispersion relation and the observation of the interference between the self-excited and driven DAWs are presented in Sec. V. A final summary and conclusions are given in Sec. IV.

II. FLUID THEORY OF THE DUST ACOUSTIC WAVE

The dust acoustic wave was first predicted theoretically by Rao *et al.*[1] in 1990. In that work, the dust acoustic wave is derived using a one-dimensional fluid approach by considering the dust continuity and momentum equations[19] shown in Eqs. (1a) and (1b),

$$\frac{\partial n_d}{\partial t} + \frac{\partial}{\partial x}(n_d v_d) = 0, \tag{1a}$$

[a)]Electronic mail: etjr@physics.auburn.edu.

$$n_d \frac{\partial v_d}{\partial t} + n_d v_d \frac{\partial v_d}{\partial x} = -\frac{n_d q_d}{m_d}\frac{\partial \varphi}{\partial x} - \frac{k_B T_d}{m_d}\frac{\partial n_d}{\partial x}. \quad (1b)$$

In Eq. (1a), n_i, n_e, and n_d are the ion, electron, and dust densities, respectively; e is the electron charge, q_d is the dust grain charge, which is assumed to be negative (which is appropriate for laboratory plasmas) and is given by $q_d=-Z_d e$ with Z_d being the number of electrons on the grain surface; m_d is the dust grain mass; k_B is Boltzmann's constant; T_d is the temperature of the dust grains; v_d is the dust velocity; and φ is the plasma potential.

For this very-low-frequency wave, we assume that the ion (n_i) and electron (n_e) densities are given by Boltzmann distributions: $n_i=n_{i0}e^{-e\varphi/k_B T_i}$ and $n_e=n_{e0}e^{e\varphi/k_B T_e}$, with electron and ion temperatures T_e and T_i, respectively. This system of equations is then closed by Poisson's equation,

$$\frac{\partial^2 \varphi}{\partial x^2} = -\frac{1}{\varepsilon_0}(en_i - en_e - q_d n_d), \quad (2)$$

where ε_0 is the permittivity of free space and φ is the plasma potential.

Equations (1) and (2) are linearized assuming no charge fluctuations, i.e., $q_d=q_{d0}=-eZ_{d0}$, no zero-order drift, $v_{d0}=0$; and, the dust density, plasma potential, and dust velocity are represented using the form $a_0+a_1\exp(-i\omega t+ikx)$, where ω is the wave frequency and k is the wave number. The resulting linear dispersion relation is

$$\omega^2 = k^2 v_{td}^2 + \frac{k^2 C_D^2}{(1+k^2\lambda_D^2)}, \quad (3)$$

where

$$C_D = \omega_{\mathrm{pd}}\lambda_D = \left(\frac{n_{d0}Z_{d0}^2 e^2}{\varepsilon_0 m_d}\right)^{1/2}\lambda_D \quad (4)$$

is the dust acoustic wave speed, $\omega_{\mathrm{pd}}=(e^2Z_d^2 n_{d0}/\varepsilon_o m_d)^{1/2}$ is the dust plasma frequency, and λ_D is the effective (linearized) Debye length calculated from the electron and ion Debye lengths $\lambda_D^{-2}=\lambda_{De}^{-2}+\lambda_{Di}^{-2}$, with $\lambda_{Dj}=(\varepsilon_o k_B T_j/q_j^2 n_j)^{1/2}$. The term v_{td} is the thermal speed of the dust, which is given by $(k_B T_d/m_d)^{1/2}$.

The result presented in Eq. (3) is the most general form of the dust acoustic wave dispersion relationship if drifts and collisions are neglected. In the vast majority of experiments, it has been assumed that the dust temperature is low (i.e., $T_d \sim 1/40$ eV) and that the second term in the equation is dominant. Furthermore, most experiments are performed in the long-wavelength limit where $k\lambda_D \ll 1$. Under those conditions, the dispersion relation simply reduces to $\omega/k=C_D$. This has been the approximation used to interpret the majority of dust acoustic wave experiments.

However, in the experiments described in Sec. III, it is shown that the simplified linear dispersion relation with room-temperature dust particles *does not* agree with the experimental measurements.

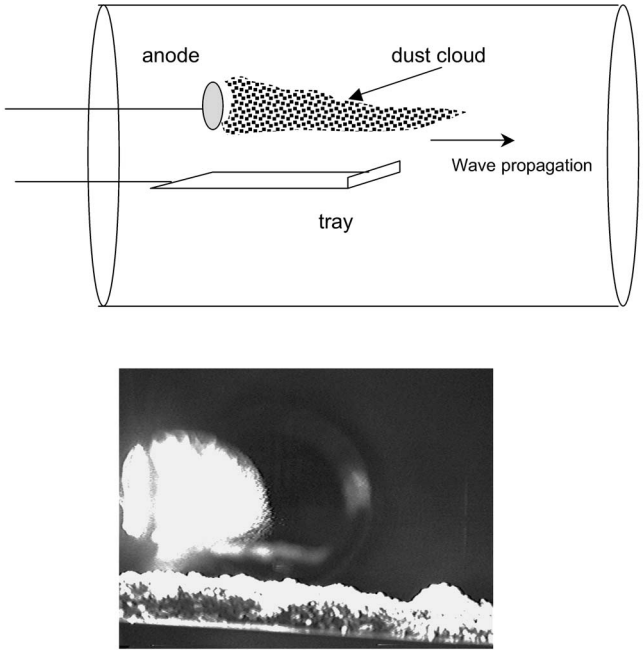

FIG. 1. Schematic and photograph of the interior of the Dusty Plasma Device (DPD). Here, the dust cloud, powder on the dust tray, and the anode are shown.

III. EXPERIMENTAL SETUP AND MEASUREMENTS

In this paper, the authors have performed a driven dust acoustic wave experiment in which the current modulation occurs at frequencies much higher ($f>100$ Hz) than those used in earlier experiments. At these frequencies, it was expected that the role of the finite $k\lambda_D$ would begin to play a role in the experimental observations. However, this transition was not observed. Instead, it will be shown that finite dust temperature effects appear to dominate the experimental results.

The experiments reported in this paper were performed on the same Dusty Plasma Device (DPD) used in the original dust acoustic wave studies by Thompson *et al.*[4] The DPD device is a 75- cm-diam, 90- cm-long cylindrical vacuum vessel. The same general experimental setup as reported in the 1997 experiment was used. Here, a 1 in. (2.5 cm) diameter anode is inserted into the chamber. An electrically floating 12- in.-long by 4–in.-wide (30 cm × 10 cm) plate is loaded with kaolin powder (mass density $\sim$2000 kg/m^3) that has a nominal diameter of ~ 1 μm. A photograph of a dust cloud in the device and a schematic drawing are shown in Fig. 1.

The anode is biased at a nominal voltage of 350–400 V at a constant current of 14 mA to produce a dc glow discharge plasma near the anode surface. This plasma is expanded to fill the chamber volume using a 60 G axial magnetic field. In the experiment reported in this paper, argon is used as the work gas as compared to nitrogen in the original experiment. The argon neutral pressure was in the range of 100–200 mTorr. Additionally, this experiment uses a 120 mW, diode pumped solid-state Nd:YAG laser operating at a wavelength of 532 nm to illuminate the particles as compared to a white light source in the original experiment.

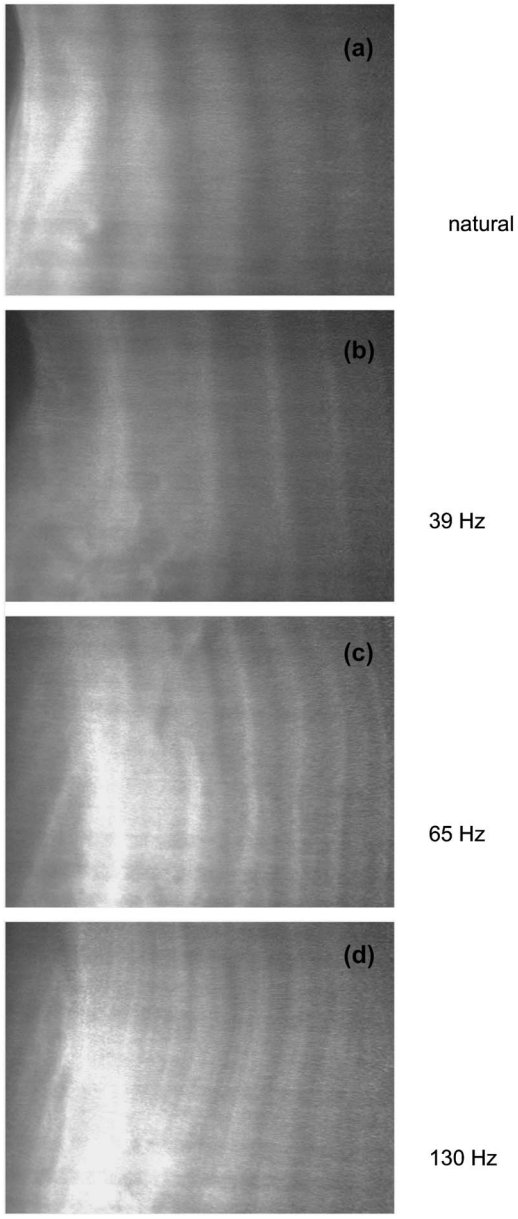

FIG. 2. A sequence of four images of dust acoustic waves in the DPD. Here, argon plasmas are generated at a pressure of 160 mTorr with an anode bias voltage of 300 V. (a) The first image is of a naturally formed dust acoustic wave. The remaining images show waves driven at different frequencies: (b) 39 Hz, (c) 65 Hz, and (d) 130 Hz.

In the experiment, the glow discharge plasma is formed with a constant bias voltage and constant current applied to the anode. Under these conditions, a dust acoustic wave appears spontaneously in the discharge. This wave starts near the anode and propagates away from the anode. Nominally, these naturally formed waves have $f \sim 47 \pm 4$ Hz and $k_{\mathrm{DAW}} \sim 22.7 \pm 2.6$ cm^{-1}. A sinusoidal modulation to the discharge current with an amplitude of 3–5 mA is then applied to the anode at frequencies ranging from $f=15$ to 150 Hz (or $\omega \sim 100$ to 1000 rad/s). As was reported in Thompson *et al.*,[4] the driven dust acoustic waves become synchronized to the current modulation allowing control over the wave frequency. In this manner, it is possible to use a video camera to record the waves and measure the wavelength. Figure 2 shows an example of several typical dust acoustic wave images for both the naturally occurring [Fig. 2(a)] and driven [Figs. 2(b)–2(d)] dust acoustic wave.

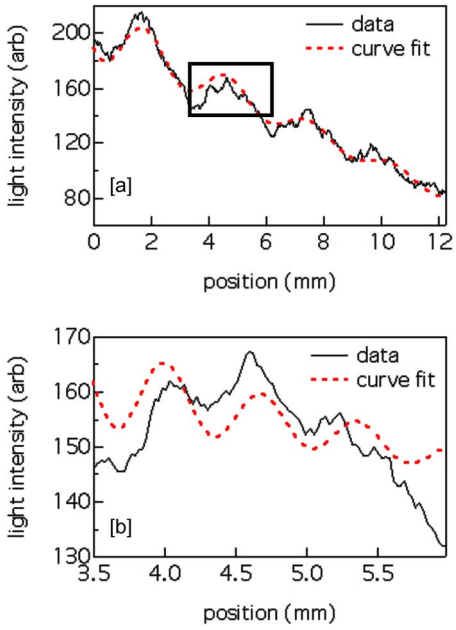

FIG. 3. (Color online) Analysis of the dust acoustic wave modulation. (a) For a horizontal "slice" through the waves, there is a clear modulation of the light intensity that corresponds to peaks and troughs of the dust acoustic wave. (b) Using the region indicated in the black box, an additional structure is observed within the main dust acoustic waves. In combination, the long-wavelength ($k_{\mathrm{long}}=26\pm2$ cm^{-1}) modulation in (a) represents the low-frequency (possibly natural dust acoustic) mode while the short-wavelength ($k_{\mathrm{short}}=77\pm8$ cm^{-1}) modulation in (b) represents the high-frequency driven mode.

IV. MEASUREMENT OF THE DISPERSION RELATION

In order to determine the dispersion relation, it is necessary to extract the wavelength of the DAWs for each applied frequency. To measure the wavelengths, a 30 frames per second digital camera is used to record a 640 pixel by 480 pixel movie of the waves for up to five seconds. The software program ImageJ[20] is used to obtain a light intensity profile for an interrogation box that is typically 200–300 pixels long (horizontally) and 50 pixels wide (vertically). The curve fit to light intensity profile is then used to extract the wavelength of the dust acoustic wave for a single video image. An example of this process is shown in Fig. 3. A sequence of 100 images is analyzed in this manner to obtain an average value of the wavelength (wave number) for each applied frequency. From the frequency and wave-number information, a plot of the dispersion relationship ω versus k can be constructed.

When this analysis was first performed, the resulting dispersion relationship had an unusual structure. This is shown in Fig. 4(a). It is noted that above a certain frequency, in this case $f>45$ Hz (or $\omega>282$ rad/s), there was no apparent change in the value of the wave number, $k \sim 27.2 \pm 6.3$ cm^{-1}. This change in the behavior of the waves appears to be related to the frequency and wave number of

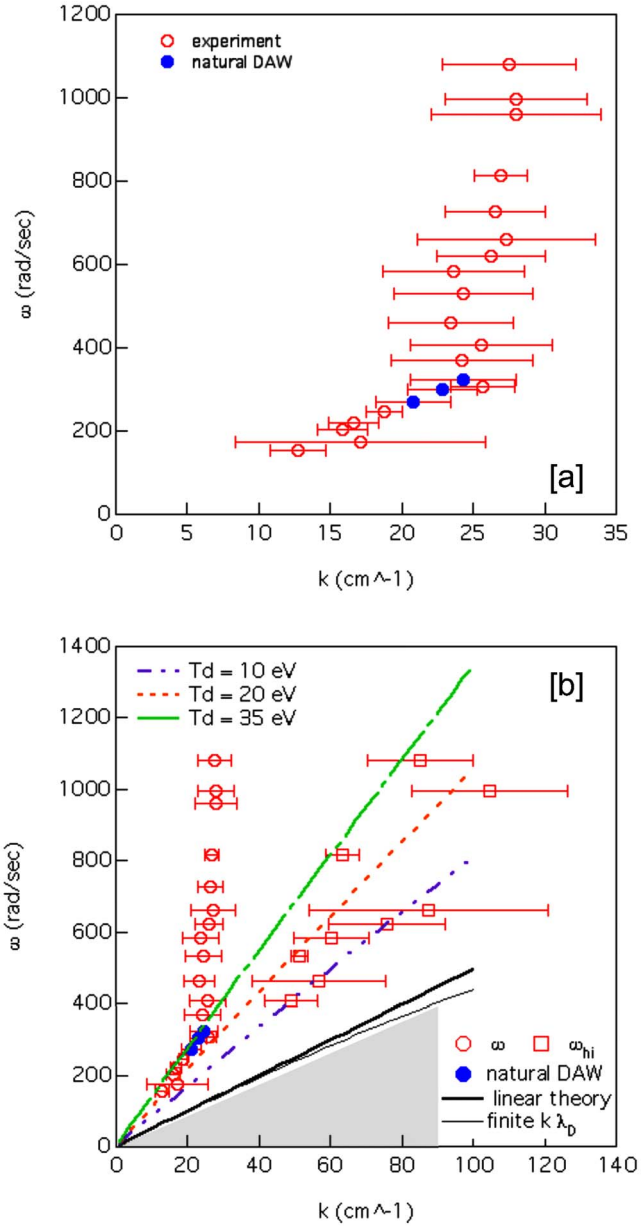

FIG. 4. (Color online) (a) Measured dispersion relationship of the "long-wavelength" structure observed in the experiment. Open circles represent measured values of the wave number for an applied modulation frequency. The solid circles represent measurements of the naturally occurring (unmodulated) dust acoustic wave. (b) Expanded version of the measured dispersion relationship that includes both the long- (open circles) and short-wavelength (open squares) observations. The solid curves represent the theoretically calculated dispersion relationship with (thin black line) and without (thick black line) the finite $k\lambda_D$ effects, but with $T_d=1/40$ eV (i.e., cold dust). The three remaining dashed curves are dispersion curves that include finite dust temperature effects for dust temperatures of 10, 20, and 35 eV.

the natural dust acoustic wave, suggesting that as the applied frequency was increased, the dust acoustic wave in the experiment appeared to "lock" to the natural wave properties. Thus, the data points in Fig. 4(a) that are vertically grouped at $k \approx 25$ cm^{-1} are not associated with the actual driving frequencies, but correspond to the naturally excited wave frequency.

However, a careful examination of Figs. 2(c) and 2(d) reveals that there is additional fine structure *within* the wave fronts. As indicated in Fig. 3(b), this fine structure can be fit using the same light intensity analysis approach as described above, but using a restricted interrogation region that is only 60–80 pixels long (horizontally) in order to resolve the details of these structures. When this analysis is performed, it becomes clear that shorter-wavelength (i.e., high wave number) collective structures, corresponding to the actual driving frequencies, are present in the dusty plasma.

As a result, when the information about the higher wave numbers is incorporated into the dispersion plot, with the continued assumption that the applied modulation frequency is responsible for the driven, short-wavelength waves, the plot is significantly modified, as shown in Fig. 4(b). Here, the original data points are plotted using circles, and the reanalyzed, high-frequency data are plotted using squares. Nonetheless, the data show the extension of the linear relationship between the angular frequency, and the wave number extends to high frequencies.

To interpret these measurements, it is necessary to make an estimate of the dust acoustic wave dispersion relation for these experimental conditions. First, a floating double probe was used to measure the background plasma parameters in the absence of the dust particles. It was found that the plasma density is $n \sim 5 \times 10^{14}$ m^{-3} and the electron temperature is $T_e \sim 2.5$ eV. It is assumed that the plasma consists of cold ions ($T_i \sim 0.025$ eV) and dust particles with an average radius of $\langle r_d \rangle \sim 0.5$ micrometers (or $m_d \sim 1.05 \times 10^{-15}$ kg). From the interparticle spacing measured from the video images, an average dust number density is estimated, $n_d \sim 1 \times 10^{11}$ m^{-3}. These parameters are used to make a self-consistent estimate of the dust grain charge, using orbit-motion limited theory, of $Z_d \sim 1800$ electrons.[19] Based upon these values and the assumption of cold, room-temperature dust particles ($T_d=1/40$ eV), the dust acoustic velocity is estimated from Eq. (3) to be $C_D=2.7$ cm/s. This curve is plotted as the thick, solid black line in Fig. 4(b).

It is noted that this solid line falls well below the experimental measurements. Furthermore, any of the expected finite Debye length effects would act to decrease the slope of the $\omega/k=$const line as indicated by the thin, solid line. Finally, if the particles are assumed to have a larger size than the $\langle r_d \rangle \sim 0.5$ micrometers (e.g., due to clumping of particles), the dispersion relation would shift downward into the gray-shaded region indicated in Fig. 4(b). This would lead to a larger disagreement between the experimental measurements and the theory.

However, if the dust is not taken to be cold, but considered to have a finite temperature, the theoretical calculations can be shown to come into agreement with the experimental data. This is shown by the three dashed lines in Fig. 4(b), each of which corresponds to an estimate of the dispersion relation for a range of dust temperatures between 10 and 35 eV using all of the experimentally determined parameters indicated above. These calculations show broad general agreement with the experimental measurements. If this interpretation is accurate, this result suggests that it may be very difficult to explore the finite Debye length effects on dust acoustic waves in a weakly coupled dusty plasma.

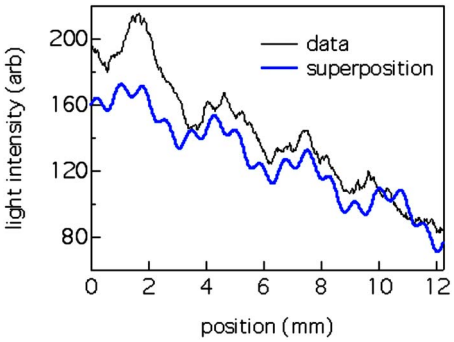

FIG. 5. (Color online) Comparison of an experimental measurement with a model [Eq. (3)] that assumes a superposition of a natural dust acoustic wave with a high-frequency driven wave.

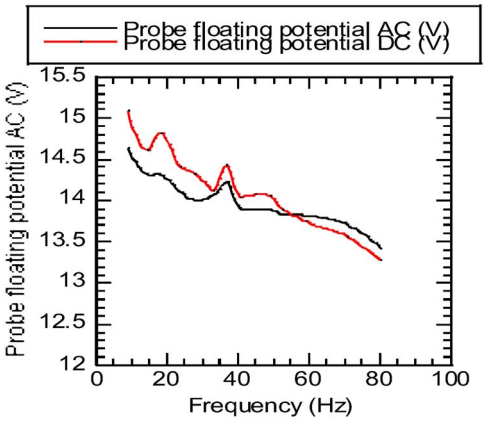

FIG. 6. Measurement of the modulation of the perturbation amplitude as a function of the applied frequency. The measurement shows that there is a decrease in the measured amplitude with increasing frequency for a fixed input amplitude.

An additional consideration for a finite value of the dust temperature can be based upon the estimate of the Coulomb coupling parameter for this experiment. The Coulomb coupling parameter, $\Gamma=(q_d^2/4\pi\varepsilon_0 k_B T_d \Delta)e^{-\Delta/\lambda_D}$, is the ratio of the electrostatic energy to the thermal energy of the microparticles. Here, Δ is the average interparticle spacing of the dust particles. Within the dusty plasma community, this is a useful parameter for characterizing the properties of the microparticle suspension. When $\Gamma \ll 1$, the system is considered to be disordered and fluid-like (weakly coupled), and when $\Gamma \gg 1$, the system is considered to be ordered and solid-like (strongly coupled).

If the dust kinetic temperature is assumed to be cold (i.e., approximately equal to the neutral temperature $\sim 1/40$ eV), then $\Gamma \sim 50-300$. Past studies have shown that for $\Gamma > 172$, the dusty plasma should exist in a Coulomb crystalline state.[21] Clearly, from Fig. 2, this system is *not* in a crystalline state. However, if the higher values of the dust temperature (~ 25 eV) are used to estimate the coupling parameter, values of $\Gamma \sim 0.05-0.3$ are obtained. These values would place the experiment clearly into the weakly coupled regime and give a result that is in good qualitative agreement with the experimental observations.

V. DISCUSSION

An outstanding question in the assessment of this work is whether the dust particles could have these high temperatures. Although the authors did not directly measure the dust temperature in this study, there is substantial supporting evidence from similar experiments that suggest that finite dust temperatures can play an important role. It is noted that numerous experiments in the recent past—though mostly in rf generated dusty plasma—have been shown to have high dust temperatures,[22,23] particularly at low neutral pressures. Moreover, these results are consistent with recent measurements by Williams[24,25] that show that dust particles in dc glow discharge dusty plasmas can have finite temperatures up to many tens of electron volts. Therefore, one likely conclusion of this work is that it may become increasingly necessary to include the effects of finite dust temperatures when the dust component is in a weakly coupled state. In fact, it may be possible that the high dust temperatures are due to the presence of an ion-dust streaming instability, as suggested by Joyce *et al.*[26]

One interesting feature of these measurements is the apparent modulation of the "natural" dust acoustic waves by the higher-frequency waves. The experimental data suggest that once the applied modulation is at a frequency larger than that of the natural dust acoustic frequency, the collective mode in the plasma gives the appearance of an amplitude modulated signal, i.e., there is a "carrier" signal at the natural dust acoustic frequency and a higher-frequency wave that "rides" on top of the carrier. In other words, there is a superposition of the driven wave and the natural dust acoustic wave.

This is illustrated in Fig. 5, where we have taken Fig. 3(a) and modeled the data as the sum of two sine waves according to Eq. (3),

$$y(x) = a_0 + a_1 \sin(k_{\mathrm{DAW}} x + \varphi) + a_2 \sin(k_{\mathrm{drive}} x) + mx, \quad (5)$$

where the function $y(x)$ is the intensity of light scattered from the microparticles. The values used for the model are $a_0=170$, $a_1=10$, $a_2=5$, $\varphi=-1.7$, $m=-7$, $k_{\mathrm{DAW}}=21$ cm^{-1}, and $k_{\mathrm{drive}}=77$ cm^{-1}. Here, k_{DAW} and k_{drive} are the wave numbers of the natural dust acoustic wave and the high-frequency driven wave, respectively; a phase shift, φ, is allowed between the two waves; and the last term mx allows for the decreasing scattered light intensity as the particles move away from the anode. The superposition model curve shown in Fig. 5 shows generally good agreement with the experimental data, giving us confidence that this may be a possible explanation for this measurement. However, the authors of this paper are not aware of any other report within the dusty plasma community of a similar phenomenon. Nonetheless, an outstanding question is why this mixture of the natural and driven waves only appears at the higher frequencies (Fig. 5).

One possible explanation is that the amplitude of the applied perturbation *in the plasma* varies as a function of

frequency. To test this, a measurement is made of the floating potential fluctuations in the plasma as a function of the applied perturbation while the wave amplitude is fixed at the signal generator. The results of this test are shown in Fig. 6. Here, it is observed that as a function of frequency, for a fixed input amplitude, the detected wave amplitude in the plasma decreases as a function of frequency. What remains unclear is whether this decrease in the wave amplitude is responsible for the observed measurements. This will be examined in a future investigation.

VI. SUMMARY AND CONCLUSIONS

In summary, the authors have presented new measurements of a dust acoustic wave in a weakly coupled, dc glow discharge dusty plasma. In this investigation, a sinusoidal modulation is applied to a biased anode. As was done in earlier works, this modulation becomes coupled to the dusty plasma facilitating an exploration of the dispersion relationship for the wave. Here, the modulation is applied at frequencies much higher than has been done in previous experiments, well in excess of 100 Hz. The resulting dispersion relations had a bifurcation. When driven at frequencies above the natural dust acoustic wave frequency, there was an apparent *linear* superposition between the natural, longer-wavelength DAWs and a shorter-wavelength driven mode, resulting in a self-organized dust density fine structure.

The presence of these short wavelengths allows an extension of the dispersion relationship to regimes of large k values. Nonetheless, at both short and long k values, it is shown that the dispersion relation deviates significantly from a simple, linear model of the dust acoustic wave that assumes cold, room-temperature dust particles. However, when finite dust temperature effects are included in the model—for $T_d \sim 10$ to 35 eV—generally good agreement is achieved between the experimental data and computed dispersion relations. Finally, it is noted that the dust temperatures are generally consistent with other recent measurements of the temperature of weakly coupled dusty plasmas. An examination of kinetic effects on the dispersion relation associated with finite dust temperatures is presently underway.

ACKNOWLEDGMENTS

The authors extend thanks to Dr. Jeremiah Williams (Wittenberg University) and Dr. Su-Hyun Kim (University of Iowa) for useful discussions about finite dust temperature effects, and to Michael Miller for invaluable technical assistance.

This work is supported by National Science Foundation Grant No. 0354938 (E.T.) and U.S. Department of Energy Grant No. DE-FG02-04ER54795 (R.L.M.).

[1] N. Rao, P. K. Shukla, and M. Y. Yu, Planet. Space Sci. **38**, 543 (1990).
[2] A. Barkan, R. L. Merlino, and N. D'Angelo, Phys. Plasmas **2**, 3563 (1995).
[3] E. Thomas, Jr., Phys. Plasmas **13**, 042107 (2006).
[4] C. Thompson, A. Barkan, N. D'Angelo, and R. L. Merlino, Phys. Plasmas **4**, 2331 (1997).
[5] H. R. Prabhakara and V. L. Tanna, Phys. Plasmas **3**, 3176 (1996).
[6] V. I. Molotkov, A. P. Nefedov, V. M. Torchinsky, V. E. Fortov, and A. G. Khrapak, JETP **89**, 477 (1999).
[7] E. Thomas, Jr. and R. L. Merlino, IEEE Trans. Plasma Sci. **29**, 152 (2001).
[8] V. E. Fortov, A. D. Usachev, A. V. Zobnin, V. I. Molotkov, and O. F. Petrov, Phys. Plasmas **10**, 1199 (2003).
[9] V. E. Fortov, O. F. Petrov, V. I. Molotkov, M. Y. Poustylnik, V. M. Torchinsky, A. G. Khrapak, and A. V. Chernyshev, Phys. Rev. E **69**, 016402 (2004).
[10] A. Piel, M. Klindworth, O. Arp, A. Melzer, and M. Wolter, Phys. Rev. Lett. **97**, 205009 (2006).
[11] T. Trottenberg, D. Block, and A. Piel, Phys. Plasmas **13**, 042105 (2006).
[12] M. Schwabe, M. Rubin-Zuzic, S. Zhdanov, H. M. Thomas, and G. E. Morfill, Phys. Rev. Lett. **99**, 095002 (2007).
[13] P. Bandyopadhyay, G. Prasad, A. Sen, and P. K. Kaw, Phys. Lett. A **368**, 491 (2007).
[14] M. Rosenberg, J. Plasma Phys. **67**, 235 (2002).
[15] I. Kourakis and P. K. Shukla, J. Plasma Phys. **71**, 185 (2005).
[16] S. Ghosh, R. Bharuthram, M. Khan, and M. R. Gupta, Phys. Plasmas **11**, 3602 (2004).
[17] J.-K. Xue, Phys. Lett. A **320**, 226 (2003).
[18] V. V. Yaroshenko, F. Verheest, and G. E. Morfill, Astron. Astrophys. **461**, 385 (2007).
[19] P. K. Shukla and A. A. Mamun, *Introduction to Dusty Plasma Physics* (Institute of Physics Publishing, London, 2002), p. 94.
[20] W. S. Rasband, ImageJ, U.S. National Institutes of Health, Bethesda, MD, http://rsb.info.nih.gov/ij/, 1997–2006.
[21] H. Thomas, G. E. Morfill, V. Demmel, J. Goree, B. Feuerbacher, and D. Möhlmann, Phys. Rev. Lett. **73**, 652 (1994).
[22] Y. Ivanov and A. Melzer, Phys. Plasmas **12**, 072110 (2005).
[23] H. M. Thomas and G. E. Morfill, Nature **379**, 806 (1996).
[24] J. Williams and E. Thomas, Jr., Phys. Plasmas **13**, 063509 (2006).
[25] J. Williams, Doctoral dissertation, Auburn University (2006).
[26] G. Joyce, M. Lampe, and G. Ganguli, Phys. Rev. Lett. **88**, 095006 (2002).